

The QCD potential

Antonio Vairo

*Dipartimento di Fisica dell'Università di Milano and INFN, via Celoria 16, 20133 Milano, Italy
IFIC, Universitat de València-CSIC, Apt. Correus 22085, E-46071 València, Spain*

Abstract. After reviewing the definition of the heavy quark-antiquark potential in pNRQCD, we discuss recent advances in the calculation.

Keywords: effective field theories, pNRQCD, potential, perturbative QCD, lattice

PACS: 12.38.-t, 12.38.Bx, 12.38.Gc, 12.39.Hg

DEFINITION

The potential between a heavy quark and antiquark has been one of the first quantities to be studied in QCD: it is a privileged object for exploring the interplay of perturbative and non-perturbative QCD and the set in of confinement, and it plays a central role in quarkonium physics [1]. Nowadays, the progress of perturbative and lattice calculations requires an accurate and rigorous definition of the potential in QCD, phenomenological and intuitive characterizations being no longer adequate.

So, what is the QCD potential between a quark and antiquark with a large mass m ? One may first answer that the potential is the function V into the Schrödinger equation describing the quark-antiquark bound state ϕ :

$$E \phi = \left(\frac{p^2}{m} + V \right) \phi, \quad (1)$$

p being the momentum of the quark-antiquark pair in the centre-of-mass system and E its binding energy. Clearly, if Eq. (1) comes from a systematic expansion of QCD, it arises from at least a double expansion in p/m or rm (r being the inter-quark distance) and in Er . Hence, rather than Eq. (1), we may expect that the QCD expansion would lead to

$$E \phi = \left(\frac{p^2}{m} + V^{(0)}(r) + \frac{V^{(1)}(r)}{m} + \dots \right) \phi, \quad (2)$$

where the \dots stand both for terms suppressed in the non-relativistic expansion in p/m or rm and for terms suppressed in Er , sometimes referred to as retardation effects (an example is the Lamb-shift). The above double expansion becomes an expansion in the heavy-quark velocity v once we note that in a non-relativistic system $1/r \sim p \sim mv$, and $E \sim mv^2$, with $v \ll 1$.

How do the scales mv and mv^2 originate in QCD? Let's consider the case of weakly-coupled bound states, i.e. states such that Λ_{QCD} is smaller than any of the scales m , mv or mv^2 . For these states we may use perturbation theory. Near threshold, the momenta

$$\alpha_s (1 + \alpha_s/v + \dots) \approx \frac{1}{E - \left(\frac{p^2}{m} + V\right)}$$

FIGURE 1. Resummed propagator near threshold.

of the quarks are small compared to their masses, so that $p/m \sim v \ll 1$. Moreover, for certain sets of graphs, like those in Fig. 1, the perturbative expansion breaks down when $\alpha_s \sim v$. The summation of all α_s/v contributions leads to the appearance of a bound-state pole of order $mv^2 \sim m\alpha_s^2$ in the resummed propagator.

These scales get entangled in a typical amplitude. An example is provided by the annihilation diagram of Fig. 2. Assuming that the incoming quarks are near threshold, the different gluons entering the diagram are characterized by different scales. The annihilation gluons have a typical energy of order m , sometimes also called “hard scale”; binding gluons, also called “soft”, have the momentum of the incoming quarks, which is of order mv , and “ultrasoft” gluons, sensitive to the intermediate bound state, have energies of the order of the binding energy, i.e. mv^2 .

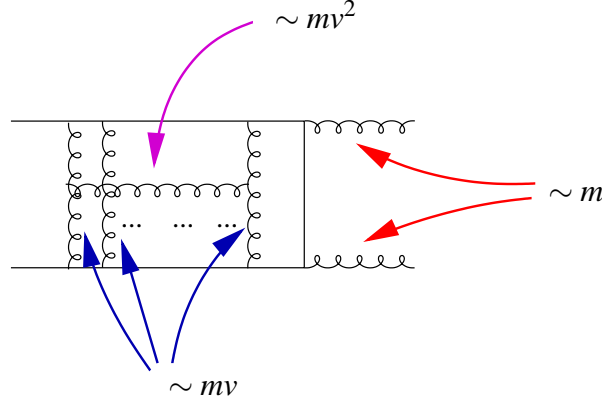


FIGURE 2. Annihilation diagram contributing to the quarkonium decay width.

In order to disentangle the different scales, it is convenient to enforce an expansion in the ratios of low-energy scales over large-energy scales at the Lagrangian level; this corresponds to substituting QCD with low-energy Effective Field Theories (EFTs) [2]. The ultimate EFT that follows from QCD by integrating out all energy scales but mv^2 is potential NRQCD (pNRQCD). The general form of the Lagrangian density of pNRQCD is

$$\mathcal{L} = \int d^3r S^\dagger \left(i\partial_0 - \frac{p^2}{m} - V_s^{(0)}(r, \mu) - \frac{V_s^{(1)}(r, \mu)}{m} + \dots \right) S + \text{ultrasoft contributions}, \quad (3)$$

where S stands for a color-singlet quarkonium field, μ is the cut-off of the EFT, and “ultrasoft contributions” include all degrees of freedom which are ultrasoft (they may be

gluons, or light quarks or other degrees of freedom). The ultrasoft contributions are typically suppressed with respect to the part of the pNRQCD Lagrangian displayed in Eq. (3). Hence, the equation of motion of the color-singlet quarkonium field is exactly Eq. (2) and we may identify $V^{(0)}(r, \mu) + V^{(1)}(r, \mu)/m + \dots$ with the heavy-quark potential.

In summary, EFTs provide the following definition of the potential: the potential is a Wilson coefficient of the EFT obtained by integrating out all degrees of freedom but the ultrasoft ones, it undergoes renormalization, develops a scale dependence and satisfies renormalization group equations, which eventually allow to resum potentially large logarithms.

THE PERTURBATIVE POTENTIAL

We consider the static potential $V_s^{(0)}$. This is obtained by integrating out soft gluons from static QCD. Soft gluons are those associated with the scale $1/r$. At short distances, $1/r \gg \Lambda_{\text{QCD}}$, soft gluons may be calculated in perturbation theory. If also the ultrasoft scale, i.e. the potential itself, is larger than Λ_{QCD} , then, besides the color-singlet quarkonium field, ultrasoft degrees of freedom include ultrasoft gluons and the color-octet quarkonium field. The matching leading QCD to pNRQCD may be done in perturbation theory, see Fig. 3. Sometimes it may be useful to choose the QCD Green's function in a gauge invariant fashion. A popular choice is the static Wilson loop.

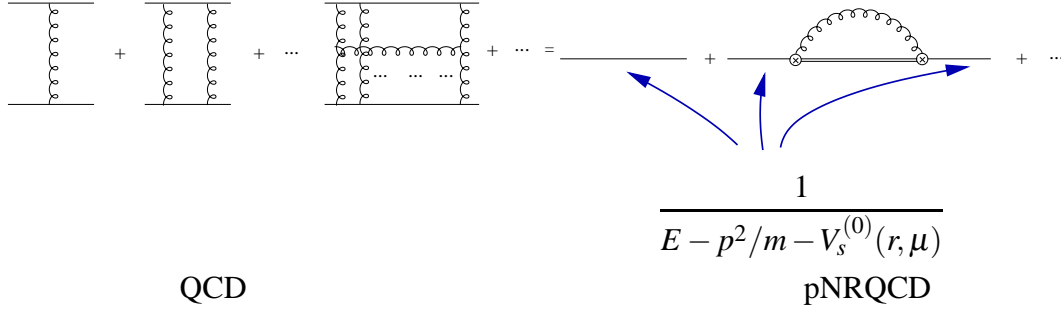


FIGURE 3. Matching condition for pNRQCD. On the left-hand side the four-fermion Green's function in QCD, on the right-hand side the singlet propagator and the first ultrasoft correction in pNRQCD. The single continuous line stands for a singlet propagator, the double line for an octet propagator and the curly line for a chromoelectric correlator. The coupling of the gauge fields with the quarkonium (circle with a cross) is a chromoelectric dipole vertex.

The matching fixes the potential and the other Wilson coefficients of the EFT. The matching condition for the singlet static potential reads

$$\lim_{T \rightarrow \infty} \frac{i}{T} \ln \langle \square \rangle = V_s^{(0)}(r, \mu) - i \frac{g^2}{N_c} V_A^2 \frac{r^2}{3} \int_0^\infty dt e^{-it(V_o^{(0)} - V_s^{(0)})} \langle \text{Tr}(\mathbf{E}(t) \cdot \mathbf{E}(0)) \rangle(\mu) + \dots, \quad (4)$$

where the box stands for the static Wilson loop of dimension $r \times T$, $V_o^{(0)}$ for the static octet potential, V_A for the electric-dipole matching coefficient, \mathbf{E} for the chromoelectric

field and $N_c = 3$ for the number of colors. The left-hand side of Eq. (4) is known at two loops [3, 4, 5, 6]. At three loops the static Wilson loop contains a term proportional to $\alpha_s^4/r \times \ln \alpha_s$, which has been calculated in [7, 8].

In order to determine the matching coefficients $V_o^{(0)}$ and V_A that enter in Eq. (4) besides $V_s^{(0)}$, we need two further matching conditions. The static octet potential $V_o^{(0)}$ has been calculated up to two loops by matching it to a static Wilson loop with color matrices in the initial and final states [9]. This gives rise to a matching condition similar to Eq. (4) [8]:

$$\lim_{T \rightarrow \infty} \frac{i}{T} \ln \langle \text{Wilson Loop} \rangle = V_o^{(0)}(r, \mu) + \dots \quad (5)$$

The matching for V_A is described in Fig. 4; it gives

$$V_A(r, \mu) = 1 + O(\alpha_s^2). \quad (6)$$

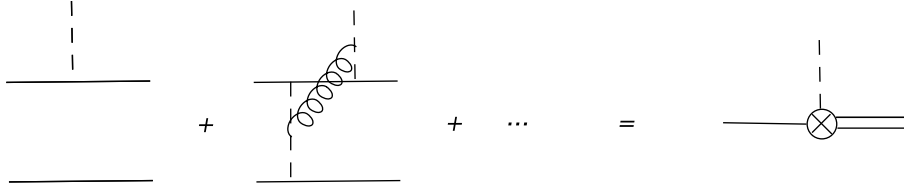


FIGURE 4. Matching condition for V_A .

The last ingredient needed in order to calculate Eq. (4) is the chromoelectric correlator $\langle \text{Tr}(\mathbf{E}(t) \cdot \mathbf{E}(0)) \rangle$, where Wilson lines connecting the chromoelectric fields are understood. This has been calculated at order α_s in [10].

Since the static Wilson loop is fully known at two loops, the matching condition (4) provides the static singlet potential at two loops. Moreover, since the static Wilson loop is independent of μ , the right hand-side of Eq. (4) should also be μ -independent. Therefore, the logarithmic dependence of the static potential may be extracted by noting that the $\ln r\mu$, $\ln^2 r\mu$, ... terms in $V_s^{(0)}$ have to cancel against the $\ln(V_o^{(0)} - V_s^{(0)})/\mu$, $\ln^2(V_o^{(0)} - V_s^{(0)})/\mu$, ... $\ln r\mu$, $\ln^2 r\mu$, ... terms in $\int_0^\infty dt e^{-it(V_o^{(0)} - V_s^{(0)})} \langle \text{Tr}(\mathbf{E}(t) \cdot \mathbf{E}(0)) \rangle$. This leads to a great simplification in the calculation of the logarithmic dependence of the static potential: the logarithmic contribution at N³LO and the single logarithmic contribution at N⁴LO may be extracted respectively from a one-loop and two-loop calculation in the EFT. Finally, we note that the solutions of the renormalization group equations allow the calculation and resummation of all logarithmic contributions of a given type (e.g. leading logarithms of the type $\alpha_s^3 \times (\alpha_s \ln \mu r)^n$, next-to-leading logarithms of the type $\alpha_s^4 \times (\alpha_s \ln \mu r)^n$ and so on).

The presently most accurately known fixed-order expression of the static singlet potential is

$$\begin{aligned}
V_s^{(0)}(r, \mu) = & -C_F \frac{\alpha_s(1/r)}{r} \left\{ 1 + \frac{\alpha_s(1/r)}{4\pi} [a_1 + 2\gamma_E \beta_0] \right. \\
& + \left(\frac{\alpha_s(1/r)}{4\pi} \right)^2 \left[a_2 + \left(\frac{\pi^2}{3} + 4\gamma_E^2 \right) \beta_0^2 + 2\gamma_E (2a_1 \beta_0 + \beta_1) \right] \\
& + \left(\frac{\alpha_s(1/r)}{4\pi} \right)^3 \left[\frac{16\pi^2}{3} C_A^3 \ln r\mu + \tilde{a}_3 \right] \\
& \left. + \left(\frac{\alpha_s(1/r)}{4\pi} \right)^4 \left[a_4^{L2} \ln^2 r\mu + \left(a_4^L + \frac{16}{9} \pi^2 C_A^3 \beta_0 (-5 + 6 \ln 2) \right) \ln r\mu + \tilde{a}_4 \right] \right\}, \quad (7)
\end{aligned}$$

where $C_F = T_F(N_c^2 - 1)/N_c$, $C_A = N_c$, $T_F = 1/2$, $\beta_0 = 11C_A/3 - 4T_F n_f/3$, $\beta_1 = 34C_A^2/3 - 20C_A T_F n_f/3 - 4C_F T_F n_f$, n_f is the number of (massless) flavors, γ_E is the Euler constant and α_s is the strong coupling constant in the $\overline{\text{MS}}$ scheme. The coefficients a_1 , a_2 , a_4^{L2} and a_4^L stand for

$$a_1 = \frac{31}{9} C_A - \frac{20}{9} T_F n_f, \quad (8)$$

$$\begin{aligned}
a_2 = & \left(\frac{4343}{162} + 4\pi^2 - \frac{\pi^4}{4} + \frac{22}{3} \zeta(3) \right) C_A^2 - \left(\frac{1798}{81} + \frac{56}{3} \zeta(3) \right) C_A T_F n_f \\
& - \left(\frac{55}{3} - 16\zeta(3) \right) C_F T_F n_f + \left(\frac{20}{9} T_F n_f \right)^2, \quad (9)
\end{aligned}$$

$$a_4^{L2} = -\frac{16\pi^2}{3} C_A^3 \beta_0, \quad (10)$$

$$\begin{aligned}
a_4^L = & 16\pi^2 C_A^3 \left[a_1 + 2\gamma_E \beta_0 + T_F n_f \left(-\frac{40}{27} + \frac{8}{9} \ln 2 \right) \right. \\
& \left. + C_A \left(\frac{149}{27} - \frac{22}{9} \ln 2 + \frac{4}{9} \pi^2 \right) \right]. \quad (11)
\end{aligned}$$

The coefficient a_1 was calculated in [11], the coefficient a_2 in [3, 4, 5, 6], the term proportional to $\alpha_s^4/r \times \ln r\mu$ in [7, 8], the coefficient a_4^{L2} in [12, 13] and the coefficient a_4^L in [13]. The coefficients \tilde{a}_3 and \tilde{a}_4 are only partially known (see [13] for discussion and references). The leading logarithmic contributions have been resummed to all orders in [12].

Expression (7) shows explicitly the Wilson coefficient nature of the static potential. It shows a scale dependence, which comes from the renormalization, and it satisfies renormalization group equations, which allow to resum potentially large $\ln r\mu$ terms. Also large contributions of the renormalon type may be analyzed in the EFT framework.

By summing Eq. (7) to the ultrasoft contributions we get back the static Wilson loop, i.e. the energy between two static sources in QCD. This reads

$$\begin{aligned}
E_0(r) = & -\frac{C_F \alpha_s(1/r)}{r} \left\{ 1 + \frac{\alpha_s(1/r)}{4\pi} [a_1 + 2\gamma_E \beta_0] \right. \\
& + \left(\frac{\alpha_s(1/r)}{4\pi} \right)^2 \left[a_2 + \left(\frac{\pi^2}{3} + 4\gamma_E^2 \right) \beta_0^2 + 2\gamma_E (2a_1 \beta_0 + \beta_1) \right] \\
& + \left(\frac{\alpha_s(1/r)}{4\pi} \right)^3 \left[\frac{16\pi^2}{3} C_A^3 \ln \frac{C_A \alpha_s(1/r)}{2} + \tilde{a}'_3 \right] \\
& \left. + \left(\frac{\alpha_s(1/r)}{4\pi} \right)^4 \left[a_4^{L2} \ln^2 \frac{C_A \alpha_s(1/r)}{2} + a_4^L \ln \frac{C_A \alpha_s(1/r)}{2} + \tilde{a}'_4 \right] \right\}. \quad (12)
\end{aligned}$$

This quantity may be compared with the short-distance behaviour of the static Wilson loop provided by lattice calculations, see for instance [14, 15].

THE NON-PERTURBATIVE POTENTIAL

At large distances, $1/r \sim \Lambda_{\text{QCD}}$, due to confinement, ultrasoft effective degrees of freedom may only be colorless objects. If Goldstone bosons are neglected, the color-singlet quarkonium field S turns out to be the only dynamical degree of freedom at scales lower than Λ_{QCD} [8]. The static singlet potential is then simply given by

$$V_s^{(0)} = \lim_{T \rightarrow \infty} \frac{i}{T} \ln \langle \square \rangle. \quad (13)$$

A recent lattice determination is shown in Fig. 5.

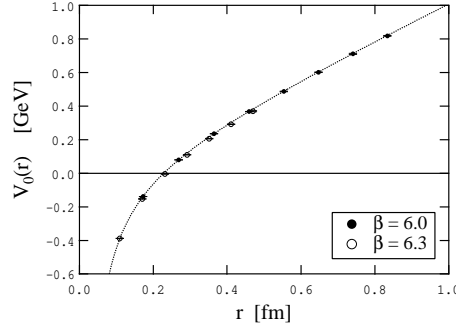


FIGURE 5. Lattice determination of the right-hand side of Eq. (13), from [16].

Recently, and for the first time, the leading relativistic correction to the static potential has been calculated on the lattice. The existence of a possibly large non-perturbative $1/m$ potential, $V_s^{(1)}$, was first pointed out in [17]. $V_s^{(1)}$ may be written as a static Wilson loop with two chromoelectric field insertions on the same quark line:

$$\frac{V_s^{(1)}}{m} = -\frac{1}{2m} \int_0^\infty dt t \langle \square^E \rangle. \quad (14)$$

The corresponding lattice determination is shown in Fig. 6.

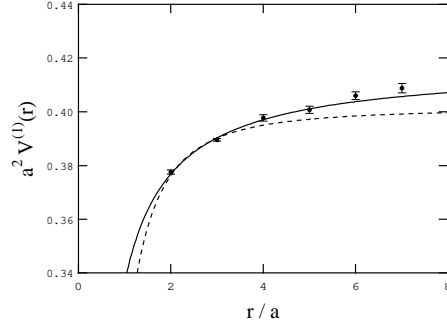


FIGURE 6. Lattice determination of the right-hand side of Eq. (14), from [18].

Note that, in accordance to power counting arguments, in the long-range, the $1/m$ potential may be as large as the static potential and contribute with it to the leading-order potential [17].

By the same collaboration, spin-dependent $1/m^2$ potentials have been calculated on the lattice with unprecedented precision. Expressions for the spin-dependent potentials in terms of static Wilson loops and field-strength insertions have been derived in [19, 20]. These have been used to obtain the lattice results shown in Fig. 7.

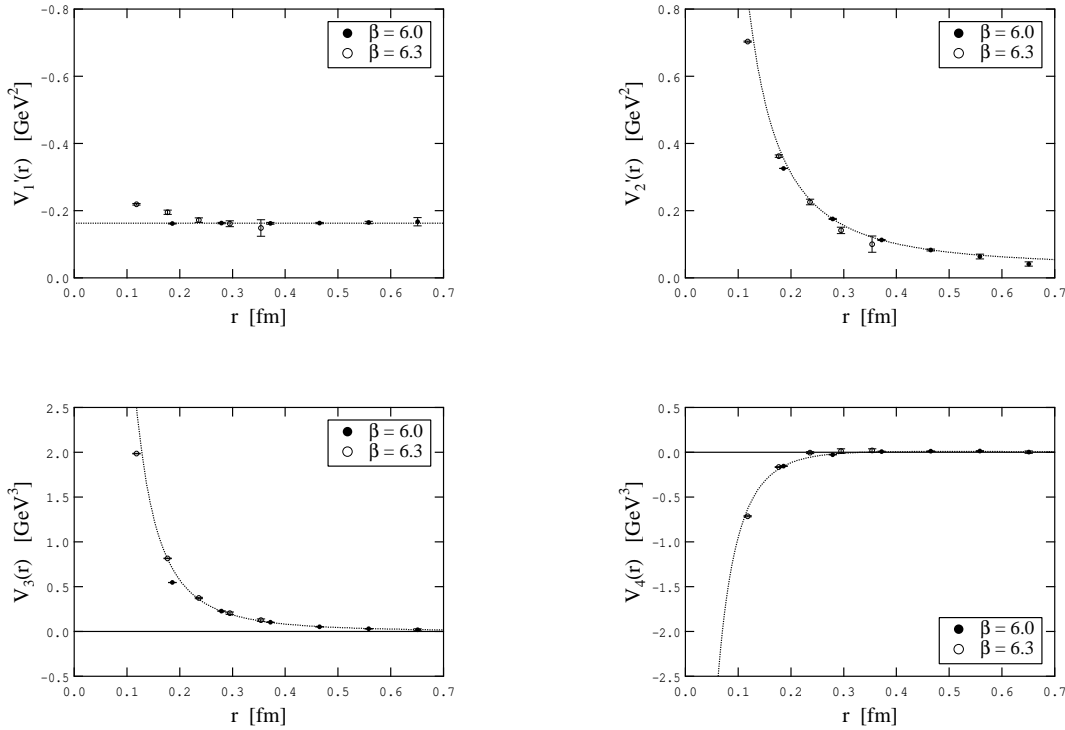


FIGURE 7. Lattice determination of the spin-dependent $1/m^2$ potentials, from [16]. The potentials V'_1 and V'_2 are spin-orbit potentials, the potential V_3 is the tensor potential and the potential V_4 the spin-spin potential.

In the long range, the spin-orbit potentials show, for the first time, deviations from the flux-tube picture of chromoelectric confinement. Since a fully consistent renormal-

ization of the EFT operators is still missing in the lattice analysis, it may be premature to draw any definitive conclusion. However, progress has been made recently in this direction. In [21], the non-perturbative renormalization of the chromomagnetic operator in the Heavy Quark Effective Theory, which crucially enters in all spin-dependent potentials, has been performed for the first time. A proper operator renormalization is also crucial in order to verify an exact relation among the spin-dependent potentials required by Lorentz invariance [22, 23], which was checked in [16] at the few percent level.

CONCLUSIONS

Non-relativistic EFTs provide a rigorous definition of the potential between a heavy quark and antiquark (see [24] for systems made by two or three heavy quarks). In the perturbative regime, the potential is a key ingredient for precision calculations of several threshold observables. In the non-perturbative regime, it can be calculated on the lattice; the corresponding EFT, pNRQCD, may provide lattice studies with an alternative to more traditional EFTs with heavy quarks, like NRQCD.

ACKNOWLEDGMENTS

The author acknowledges the financial support obtained inside the Italian MIUR program “incentivazione alla mobilità di studiosi stranieri e italiani residenti all’estero” and by the European Commission MRTN FLAVIA*net* [MRTN-CT-2006-035482].

REFERENCES

1. N. Brambilla *et al.*, *Heavy quarkonium physics*, CERN-2005-005 [arXiv:hep-ph/0412158].
2. N. Brambilla, A. Pineda, J. Soto and A. Vairo, *Rev. Mod. Phys.* **77** (2005) 1423.
3. M. Peter, *Phys. Rev. Lett.* **78** (1997) 602.
4. M. Peter, *Nucl. Phys. B* **501** (1997) 471.
5. Y. Schröder, *Phys. Lett. B* **447** (1999) 321.
6. B. A. Kniehl, A. A. Penin, M. Steinhauser and V. A. Smirnov, *Phys. Rev. D* **65** (2002) 091503.
7. N. Brambilla, A. Pineda, J. Soto and A. Vairo, *Phys. Rev. D* **60** (1999) 091502.
8. N. Brambilla, A. Pineda, J. Soto and A. Vairo, *Nucl. Phys. B* **566** (2000) 275.
9. B. A. Kniehl *et al.*, *Phys. Lett. B* **607** (2005) 96.
10. M. Eidemüller and M. Jamin, *Phys. Lett. B* **416** (1998) 415.
11. A. Billoire, *Phys. Lett. B* **92** (1980) 343.
12. A. Pineda and J. Soto, *Phys. Lett. B* **495** (2000) 323.
13. N. Brambilla, X. Garcia i Tormo, J. Soto and A. Vairo, *Phys. Lett. B* **647** (2007) 185.
14. S. Necco and R. Sommer, *Nucl. Phys. B* **622** (2002) 328.
15. A. Pineda, *J. Phys. G* **29** (2003) 371.
16. Y. Koma and M. Koma, *Nucl. Phys. B* **769** (2007) 79.
17. N. Brambilla, A. Pineda, J. Soto and A. Vairo, *Phys. Rev. D* **63** (2001) 014023.
18. Y. Koma, M. Koma and H. Wittig, *Phys. Rev. Lett.* **97** (2006) 122003.
19. E. Eichten and F. Feinberg, *Phys. Rev. D* **23** (1981) 2724.
20. A. Pineda and A. Vairo, *Phys. Rev. D* **63** (2001) 054007 [Erratum-ibid. *D* **64** (2001) 039902].
21. D. Guazzini, H. B. Meyer and R. Sommer [ALPHA Collaboration], arXiv:0705.1809 [hep-lat].
22. D. Gromes, *Z. Phys. C* **26** (1984) 401.
23. N. Brambilla, D. Gromes and A. Vairo, *Phys. Lett. B* **576** (2003) 314.
24. N. Brambilla, A. Vairo and T. Röscher, *Phys. Rev. D* **72** (2005) 034021.